Biological treatment removal of rare earth elements and yttrium (REY) and metals from actual acid mine drainage

E. W. Nogueira, F. M. Licona, L. A. G. Godoi, G. Brucha and M. H. R. Z. Damianovic

ABSTRACT

Actual acid mine drainage (AMD) containing a high concentration of sulfate (~1,000 mg·L^{-1}), dissolved metals, uranium, rare earth elements and yttrium (REY) was treated using a down-flow fixed-structured bed biological reactor (DFSBR). The reactor was operated in a continuous flow mode for 175 days and the temperature was maintained at 30 °C. The synthetic AMD was gradually replaced by the actual AMD in 20, 50 and 75% of the total medium volume. Sugarcane vinasse was used as the electron donor and the influent pH of the reactor was decreased from 6.9 to 4.6 until the system collapsed. REY elements and transition metals were removed from the actual AMD and precipitated in the down-flow fixed-structured bed reactor. Sulfate reduction achieved 67 ± 22% in Phase II and chemical oxygen demand (COD) removal was above 56% in Phases I and II. Removal of La, Ce, Pr, Nd, Sm and Y was higher than 70% in both Phases II and III while Fe, Al, Si and Mn were removed with efficiencies of 79, 67, 48 and 25%, respectively. The results highlighted the potential use of DFSBR in the treatment of AMD, providing possibilities for simultaneous sulfate reduction and metal and REY recovery in a single unit.

Key words | acid mine drainage, down-flow fixed-structured bed bioreactor, metal precipitation, rare earth elements and yttrium, sulfate reduction

E. W. Nogueira (corresponding author)
L. A. G. Godoi
M. H. R. Z. Damianovic
Biological Processes Laboratory (LPB), São Carlos School of Engineering (EESC),
University of São Paulo (USP),
Av. João Dagnone, 1100, Santa Angelina, São Carlos, São Paulo 13563-120,
Brazil
E-mail: *eliswn@usp.br*

F. M. Licona
G. Brucha
Universidade Federal de Alfenas, Rodovia José Aurélio Vilela, 11999 (BR 267 Km 533) Cidade Universitária,
Poços de Caldas, Minas Gerais,
Brazil

INTRODUCTION

Acid mine drainage (AMD) is a serious environmental problem that affects aquatic and terrestrial ecosystems, as well as human health. AMD is characterized as acidic wastewater with high concentrations of sulfate and various metals (Johnson & Hallberg 2005). The problems associated with poor disposal of AMD and the lack of treatment, as well as the recovery of metals, pose an environmental challenge that can be made worse by major disasters such as the one in Mariana-MG, Brazil (Hatje *et al.* 2017).

Among the many challenges in treating AMD is the large amount of drainage generated in deactivated mines, which requires technological alternatives able to integrate economic and environmental solutions to limit the extensive damage caused by AMD releases into the soil. The flow rate of AMD generation in a lake called BF4, located in Caldas (Minas Gerais state, Brazil) at *Indústrias Nucleares do Brasil* (INB), as an example, can reach 160 m^3·h^{-1} during the wet season. First described by Miekeley *et al.* (1992), due to the low pH of around 3, such AMD is characterized by a high concentration of dissolved metals including rare earth elements and yttrium (REY), which may range from 0.5 to 71 mg·L^{-1}.

Due to the widespread use of REY in various technological applications and the high demand for these elements by countries such as China, which now owns most of the REY production, there is a high demand for these elements in the world, thus increasing their economic value (Schlinkert & van den Boogaart 2015). The presence of REY is also abundant in several other types of AMD and the lower the pH of such wastewater, the higher the concentration of REY and metals, such as Al, Mn, Cu and Zn, released into the water (Cravotta 2008; Stewart *et al.* 2017).

According to Zhao *et al.* (2007), the speciation modeling for the AMD samples indicated that the REY-sulfate complexes are the main form of dissolved REY concentration in mine waters, representing more than 60% of the total amount, followed by a free metal species form.

As the AMD's physicochemical treatment strategies are generally associated with high chemical costs, especially hydroxides for neutralization (Johnson & Hallberg 2005),

doi: 10.2166/wst.2019.398

anaerobic technology-based biological treatment has been widely proposed, integrating low costs, chemical inputs and possibly the recovery of metals from wastewater as metal sulfides (Lewis 2010).

Based on the results found in the literature, the objective of this study was to evaluate the performance of the down-flow fixed-structured bed biological reactor (DFSBR) recently proposed by Godoi *et al.* (2017a), in the biological treatment of actual AMD with significant concentrations of Al, Fe, Mn, Si, U and REY, also aiming at the potential recovery of such elements.

MATERIAL AND METHODS

Bioreactor configuration

The down-flow fixed-structured bed reactor (Figure 1) used in the present study was based on the bioreactor described by Godoi *et al.* (2017a) and consisted of a bench-scale bioreactor made of acrylic material. The fixed-structure bed for biomass immobilization consisted of four vertical columns each containing 13 low-density polyethylene rings (Figure 2). The DFSBR was operated at 30 °C and the hydraulic retention time (HRT) varied between 16 and 18.5 h (total volume of 1.9 L). The reactor was operated for 175 days distributed in four operational phases. The biomass from an upflow anaerobic sludge blanket (UASB) treating poultry slaughterhouse waste was used to seed the support material according to the procedure previously described (Godoi *et al.* 2017a).

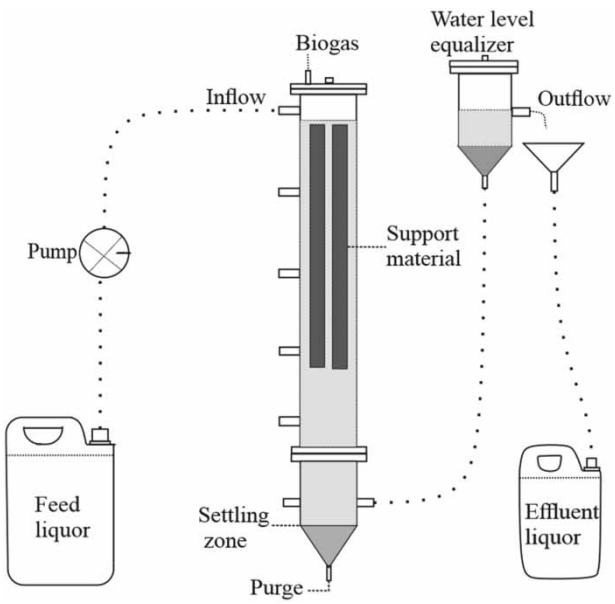

Figure 1 | Schematic representation of the down-flow fixed-structured bed reactor (DFSBR).

Figure 2 | Low-density polyethylene ring used as support material after operational time.

Mine waters

The actual AMD was collected from an acidic lake at the Osamu Utsumi Uranium Mine, deactivated in 1998 called BNF (BF4), located in Caldas (Minas Gerais state, Brazil) and operated by INB. It has been characterized by a high concentration of dissolved transition metals and the highest concentration of REY (Cravotta 2008). The pH of the mine water was around 3 and the concentration of its main elements is described in Table 1.

Electron donor

In order to provide carbon and nutrients for the sulfate-reduction metabolism, sugarcane vinasse was used as the

Table 1 | Characterization of the actual mine water used for biological treatment

Element	Conc. (mg·L^{-1})	REY	Conc. (mg·L^{-1})
Al	131.5 ± 6.6	La	40.1
Mn	75.6 ± 9.6	Ce	24.9
Fe	1.2 ± 0.1	Pr	3.6
Zn	10.9 ± 0.7	Nd	9.55
Mg	6.1 ± 0.4	U	4.15 ± 0.2
Si	17.2 ± 5.6	Y	4.10 ± 0.4
SO_4	890 ± 80		

Table 2 | Characterization of the sugarcane vinasse used as a carbon source

Analyte	Conc. ($mg{\cdot}L^{-1}$)	Analyte	Conc. ($mg{\cdot}L^{-1}$)
Al	5.84	Cu	0.366
Mn	23.28	Ti	0.228
Fe	134.1	Ni	0.204
Zn	1.48	P	147.4
Mg	1,907	SO_4	2,418
Si	53.5	Ca	1,614
		COD	$15{\cdot}10^4$

electron donor of the process. Such waste material is largely generated throughout ethanol production from sugarcane in Brazil and consisted of an organic rich effluent (Table 2). The anaerobic digestion of sugarcane vinasse has been widely reported (Gonçalves *et al.* 2007; Fuess *et al.* 2016, 2019; Nadaleti *et al.* 2019; Niz *et al.* 2019; Parsaee *et al.* 2019), and therefore its use to enable biological sulfate reduction can be considered an interesting alternative.

Operational parameters

The study was divided into four operational phases. During Phase I, the bioreactor was fed with a mixture of sugarcane vinasse and a synthetic AMD, consisting only of a high concentration of sulfate in order to develop and enrich the sulfate-reducing biomass. During Phases II, III and IV the synthetic wastewater was gradually replaced by the actual AMD until reaching 20% (Phase II), 50% (Phase III) and 75% (Phase IV) of the treated volume. The COD:Sulfate ratio applied ranged from 1.5 ± 0.4 to 2.1 ± 0.7 to provide organic matter above the stoichiometric ratio for sulfate reduction (0.67). The influent pH in the start-up phase (treating sugarcane vinasse supplemented with sulfate) was 6.9 ± 0.6, whereas after the application of the actual AMD in 75%, the influent pH was adjusted with NaOH and decreased from 5.4 to 4.6 (Table 3). The precipitated solids were collected from the bottom of the DFSBR in each operational phase to analyze the precipitated material.

Analytical methods

The concentrations of chemical oxygen demand (COD) total sulfide and alkalinity were determined according to *Standard Methods* (APHA 2005). The pH of the unfiltered samples was measured immediately after collection. Filtered samples were acidified with HNO_3 to analyze the sulfate and major elements by inductively coupled plasma optical emission spectroscopy (ICP-OES). The analytes found in the sludge accumulated in the bottom part of the bioreactor were also analyzed by ICP-OES. Detection limits were ($mg{\cdot}L^{-1}$): Al < 0.001, Fe, Mn, Sm and Y < 0.002, Si < 0.009, La < 0.005, Ce < 0.008, Pr and Nd < 0.004 and U < 0.040.

Calculations

The speciation of sulfide forms (H_2S and HS^-) and the alkalinity due to sulfide and bicarbonate in the DFSBR

Table 3 | Mean values of pH and influent of sulfate, COD and analytes in DFSBR

Phases		I (41 d)	II (18 d)	III (71 d)	IV (45 d)
Sulfate ($mg{\cdot}L^{-1}$)		980 ± 180	$1{,}150 \pm 71$	$1{,}020 \pm 70$	985 ± 144
COD ($mg{\cdot}L^{-1}$)		$1{,}530 \pm 556$	$2{,}000 \pm 111$	$1{,}980 \pm 519$	$1{,}770 \pm 450$
COD:Sulfate ratio		1.5 ± 0.4	1.7 ± 0.2	2.1 ± 0.7	1.8 ± 0.5
Influent pH		6.9 ± 0.6	5.4 ± 0.2	5.1 ± 0.1	4.6 ± 0.2
Influent ($mg{\cdot}L^{-1}$) of:	Al	–	25 ± 11	71 ± 27	96 ± 18
	Fe	–	8 ± 4	11 ± 8	6 ± 2
	Mn	–	15 ± 2	31 ± 2	62 ± 5
	Si	–	8 ± 3	12 ± 5	11 ± 2
	La	–	8 ± 4	18 ± 6	29 ± 10
	Ce	–	6 ± 3	14 ± 6	18 ± 6
	Pr	–	0.4 ± 0.3	1.0 ± 0.4	3.0 ± 0.4
	Nd	–	2 ± 1	5 ± 2	7 ± 3
	Sm	–	0.2 ± 0.1	0.6 ± 0.3	0.8 ± 0.3
	Y	–	0.8 ± 0.5	2.0 ± 0.7	3.2 ± 0.4
	U	–	1.1 ± 0.6	3.7 ± 2	3.2 ± 1.4

effluent was estimated by doing the calculations presented by Godoi *et al.* (2017b).

The flow of electrons required for the two main bioreactor metabolisms (sulfate-reduction and methanogenesis) was estimated by applying the equations reported by Godoi *et al.* (2015).

RESULTS AND DISCUSSION

COD and sulfate removal

The COD oxidation in association with sulfate reduction was successfully achieved in the first operational phase when sugarcane supplemented with sulfate was treated. In Phase I, 62 ± 14% of COD removal was observed and sulfate removal average was 54 ± 22%, reaching 87% in the last few days, indicating the establishment of the sulfate-reduction process. During Phase II, with 20% of actual AMD, COD and sulfate removal reached 56 ± 6% and 67 ± 22%, respectively (Figure 3).

Although the higher concentration of AMD did not affect the performance of the reactor at the beginning of Phase III, in the middle of this phase the COD removal dropped to 30% and was very unstable. The higher concentration of dissolved metals and low pH (around 5.0) in Phases III and IV (50% and 75% of AMD) may have seriously impaired the sulfidogenesis, leading to significant reductions in COD and sulfate removal efficiencies, close to 20% and 10% respectively.

Stoichiometrically, sulfidogenesis was responsible for the oxidation of 37, 46, 53 and 25% of the COD removed in Phases I, II, III and IV, respectively. Although the production of biogas was not measured in this study, methanogenesis seems to be an important complementary via COD removal, probably resulting in a COD/SO_4 ratio around 2, which enabled the participation of methanogenesis in the global process of organic matter removal (Godoi *et al.* 2015).

After the establishment of sulfidogenesis in the DFSBR during Phase I, the reactor presented 129 ± 12 $mg{\cdot}L^{-1}$ of total sulfide in the effluent. During Phase II, despite the lower sulfate removal efficiency observed, the increment in sulfate in the influent (Table 3) possibly stimulated the sulfate-reduction, promoting the observed increase in sulfide, which reached 210 ± 40 $mg{\cdot}L^{-1}$ (Figure 4).

In Phase III, in turn, sulfide concentration decreased to 107 ± 53 $mg{\cdot}L^{-1}$ (Figure 4). Due to low sulfate reduction, less than 20 $mg{\cdot}L^{-1}$ of sulfide was generated in the system in Phase IV, when the sulfidogenesis was severely affected and the outflow sulfate concentration remained unstable.

Once the sulfide toxicity in the biological systems was generally attributed to the molecular form (H_2S) of the hydrogen sulfide (Lens *et al.* 1998), the speciation of the sulfide forms in the liquid phase was estimated and the H_2S achieved a maximum concentration of 136 $mg{\cdot}L^{-1}$ only at day 98 of the present study. The critical threshold for sulfate-reducing bacteria (SRB), in turn, was usually expected at concentrations above 125 mg $H_2S{\cdot}L^{-1}$ (Maillacheruvu *et al.* 1993), whereas the total inhibition of sulfate-reducing metabolism was only verified at H_2S concentrations as

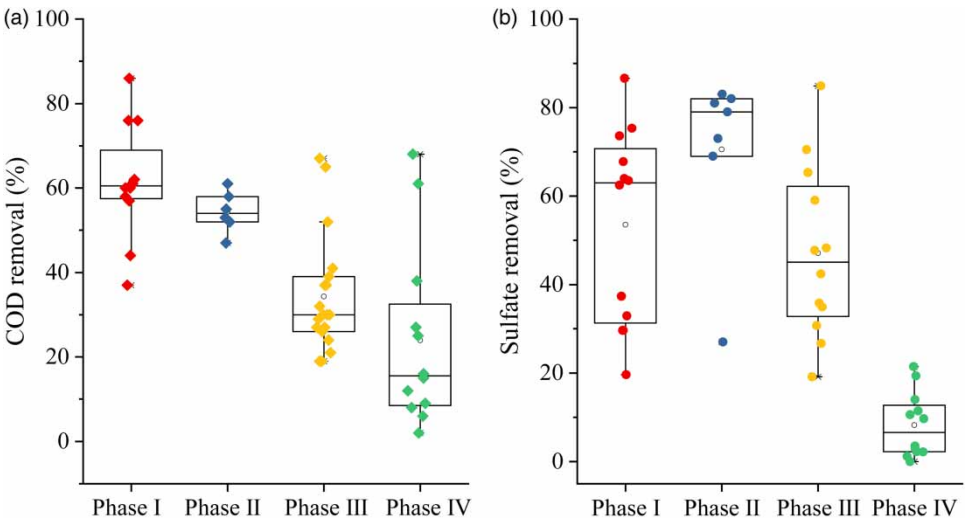

Figure 3 | Boxplot analysis of COD removal (a) and sulfate removal (b) at different phases.

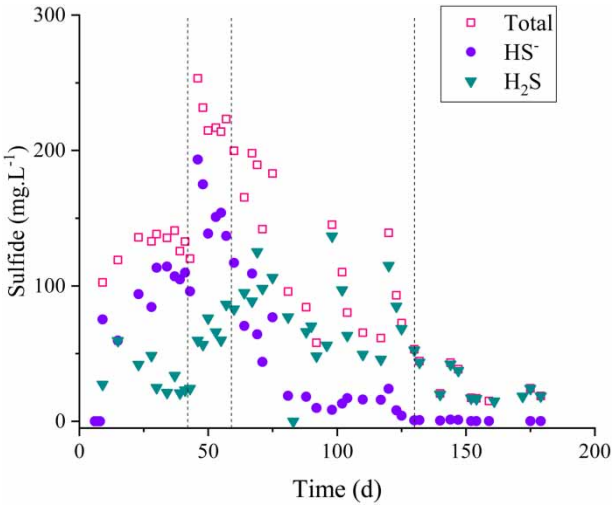

Figure 4 | Total sulfide concentration (□), bisulfide anion as HS^- (●) and hydrogen sulfide (▼).

high as 500 mg·L^{-1} (Reis *et al.* 1992). Therefore, the H_2S sulfide was maintained below this value throughout the entire operational time. Thus, the toxic effects on the sulfidogenic biomass, which may cause the observed loss of performance, should be attributed to agents other than sulfide.

The alkalinity produced increased the average pH of the system from around 7.0 to 7.5 in Phase I, 5.4 to 7.4 in Phase II, from 5.0 to 6.4 in Phase III and from 4.7 to 5.2 in Phase IV (Figure 5). In Phase I (absence of dissolved metals), 1,456 ± 190 mg $CaCO_3$·L^{-1} was produced. Although the addition of AMD did not significantly affect the sulfate reduction in Phase II, the alkalinity in the effluent of the DFSBR presented a slight decrease to 1,331 ± 96 mg $CaCO_3$·L^{-1} (Figure 5). It is probably related to the release of protons caused by metal sulfide precipitation and the HS^- consumption due to metal sulfide precipitation (Godoi *et al.* 2017b). During Phase III, as the metal concentration increased and sulfate reduction efficiency decreased, alkalinity production dropped to 626 ± 219 mg $CaCO_3$·L^{-1}. The IA/PA ratio (intermediary alkalinity/partial alkalinity) increased from 0.4 ± 0.1 (Phase I and II) to 1.9 ± 1.0 in Phase III, demonstrating the instability of the anaerobic digestion after increasing the actual AMD concentration and inflow pH. Rodriguez *et al.* (2012), who analyzed the AMD collected at the same uranium mine, also reported instability in the effluent pH and alkalinity generation by sulfidogenesis. The acidity in such AMD associated with the significant increase in metals can be the major reason for the lack of efficiency observed in the system from Phase III onwards.

The accumulation of volatile fatty acids (VFA; Figure 5) through the phases operated in more acidic conditions (Phases III and IV) also suggests that the sulfate-reduction inhibition was related to the increasing concentration of the free form of acetic acid, which is more significant in pH values below 6.2 (Reis *et al.* 1992). However, this hypothesis cannot be confirmed as the acetic acid was not individually determined.

REY and metal(loid) removal from AMD

The treatment of 75% of AMD with a high content of dissolved metals was possible due to the establishment of sulfidogenesis in the first phase, in which the DFSBR was able to develop a sulfidogenic biomass cultivated in sugarcane vinasse as the electron donor and carbon and

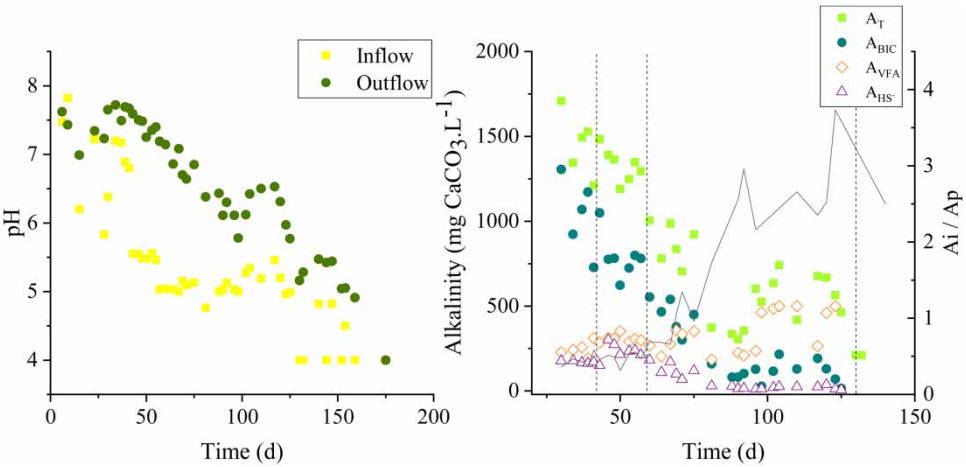

Figure 5 | Inflow (■) and outflow (●) pH (a) and total alkalinity- A_T (■) bicarbonate alkalinity- A_{BIC} (●) volatile fatty acid alkalinity- A_{VFA} (◇) and sulfide alkalinity-A_{HS}^- (△) measure as $CaCO_3$ concentration and (—) the Ai/Ap (b).

nutrient source. The removal of transition metals and REY are presented in Figures 6 and 7, respectively, and these results can also be related with the increase in the pH in the liquid medium, making precipitation of the metal(loid)s possible in the DFSBR.

Although Mn precipitates around pH 9.0 (Ayora *et al.* 2016), during Phases II and III the treatment was able to remove an average amount of 35 and 20%, respectively, when the reactor outflow pH was higher than 6.0. In Phase IV, when the pH dropped to less than 6.0, Mn was released back to the dissolved form. The incipient removal of Mn in comparison with other metals is probably due to the higher solubility product constant (Ksp) of MnS and the complexity of the interactions governing Mn solubility (Bekmezci *et al.* 2011; Santos & Johnson 2017).

The elements Al and Fe, widely associated with AMD (Sun *et al.* 2012; Ayora *et al.* 2016; Kefeni *et al.* 2017), presented similar efficiency removal of around 70% in Phases II and III but dropped in the last phase to less than 40%. Despite the similar removal efficiency, the small concentration of Fe probably precipitated as sulfide (FeS) and Al as hydroxide when the pH increased. The high concentration of dissolved sulfide probably favored the formation of metal sulfide, precipitating partially with transition metals.

According to the acid dissociation constant (pKa) of Al, pH values between 1.5 and 6.0 promote the formation of sulfate complexes of Al in AMD, and in pH values above, Al is present as hydroxide complexes (Sánchez-Espanã 2007). Falagán *et al.* (2017) also found Al in a hydroxysulfate form and other forms under pH 5.

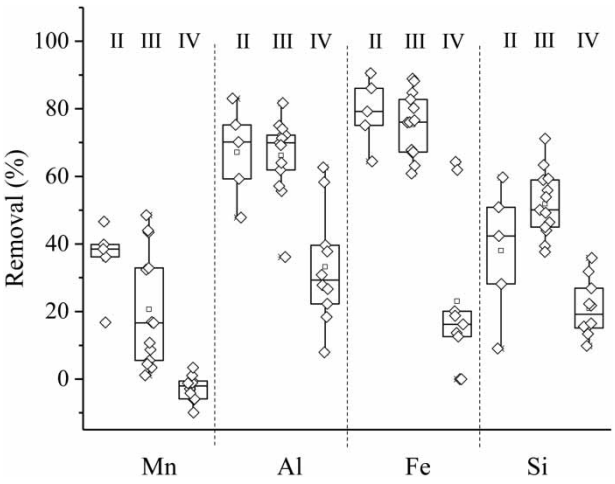

Figure 6 | Boxplot analysis of transition metals and Si metalloid removal in Phases II, III and IV.

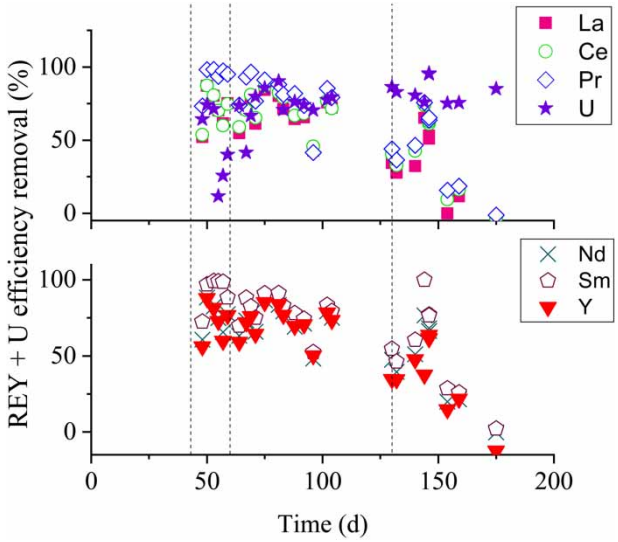

Figure 7 | REY and U removal from the dissolved fraction.

The metalloid Si is usually present in AMD as Si(OH) and they usually have the same behavior as Al because they have similar charge and ionic radii ($Al^{3+} = 0.5$ Å and $Si^{4+} = 0.47$ Å) (Caraballo *et al.* 2019). Studies suggested that Si could coprecipitate as hydrobasaluminite at pH 6 (Caraballo *et al.* 2019) and Sánchez-España *et al.* (2016, 2018) also reported the interaction between Si and Al under biotic and abiotic conditions in acidic environments.

Regarding REY, La, Ce, Nd and Y were removed in DFSBR with average efficiencies higher than 70%, while Pr and Sm presented removal efficiencies higher than 80% in Phase II (Figure 7). Compared to other AMD and coal mine drainage (CMD) with REY compositions, the DFSBR was able to treat the highest concentration of REY ever described (Miekeley *et al.* 1992; Zhao *et al.* 2007; Sun *et al.* 2012; Stewart *et al.* 2017). The obtained removal of REY suggests that they could be coprecipitated with aluminum or ferric iron (Stewart *et al.* 2017), as a metal sulfide or directly as $RE(OH)_3$ (Ziemkiewicz *et al.* 2016).

The removal of REY and metal(loid)s in DFSBR by precipitation was confirmed in each discharge of material from the conical bottom of the reactor. The analysis of the sludge indicated significant amounts of several elements (Table 4). The second chamber of the system, used as a water level equalizer (Figure 1), was also useful to retain sludge rich in precipitates (Table 4).

The highest concentration of precipitated REY was achieved for the La, which reached 696 $mg \cdot L^{-1}$ in the collected sludge. In the same sample, Al accumulated in a concentration up to 2 $g \cdot L^{-1}$. The concentration of metals

Table 4 | Concentration of precipitated elements in $mg{\cdot}L^{-1}$

Day	La	Ce	Pr	U	Nd	Sm	Y	Mn	Al	Fe	Si
57	86	67	4	n.d	23	3	9	34	243	236	41
90	245	176	20	n.d	52	6	24	80	702	135	75
137	194	136	17	5	45	5	22	87	620	87	71
110[a]	696	484	55	n.d	155	15	79	735	2,587	406	76

[a]Sample collected at the conical bottom of the water level equalizer.

detected was proportional to the value considered in the wastewater that was feeding the bioreactor. The high concentration of iron accumulated in the biomass suggests that it came from vinasse, which is also rich in Fe.

The high concentration of REY and sulfate and the low pH of actual AMD treated in the present study suggest that the main formation of dissolved REY was probably represented by the sulfate form due to its stable form. Once the sulfidogenesis was established and the internal pH increased, it made precipitation of the REY elements possible.

On the other hand, uranium's behavior differs from the other elements and its removal efficiency increased throughout the treatment. Although greater results were achieved in Phases II and III, with 75% of actual AMD, the removal efficiencies started to decline until the bioreactor collapsed (Figure 7). This collapse can be related to both inflow pH drops and a high concentration of toxic metals. Because of the down-flow configuration, the SRB can also be affected by the precipitation of the analytes of the support material, accumulating with the immobilized biomass and exerting inhibitory effects due to their toxicity to SRB, as well as by increasing the mass transfer limitation (Villa-Gomez *et al.* 2011).

Based on the concentration of REY present in the actual AMD (Table 1) and estimating that with anaerobic treatment if at least 50% of the total elements precipitated into the bioreactor, for every 100 m^3 of treated DAM 4, 1, 0.5, 0.2 kg of La, Ce, Nd and Y, respectively, could be recovered. In 2018, the price of lanthanum oxide, cerium oxide, neodymium oxide and yttrium oxide was around 2, 2, 51 and 3 US$·$kg^{-1}$, respectively (U.S. Geological Survey 2019). The price of REY can reach more than 500 times the price of iron ore, for example, and yttrium is the most valuable REY element analyzed in this study. More than 2,400 m^3 of AMD is generated per day at BF4 (just one of the four main acidic lakes disposed of at the company) and this volume is higher during the rainy seasons. INB had spent around R$1.8 mi (or US$430 thousand) buying calcium hydroxide in 2018 to increase the pH of the mine water (leaving the treatment plant with a pH higher than 11 to prevent acidic waters reaching the river) in order to comply with the Brazilian environmental laws. Although NaOH had been used in Phase IV, it was used in a small concentration just to keep the inflow pH around 4.8 in order not to affect the sulfidogenesis and it was not added to completely neutralize the medium. The abiotic remediation system not only has a high operational cost but also the generation of sludge produced by physicochemical treatment is much higher when compared with biological treatments (Johnson & Hallberg 2005). In addition to the environmental advantages, biological treatments also have economic benefits and are promising in terms of recovering valuable elements from AMD as the precipitated material is more stable.

CONCLUSION

The wastewater vinasse used as a carbon source for the biological treatment of actual AMD enabled the sulfidogenesis in the bioreactor. The alkalinity generated by sulfidogenesis was able to increase the pH in at least one unit and promoted the removal of metal(loid)s Al, Fe, Mn, Si, U and REY elements from the dissolved phase. The chemical elements precipitated and accumulated in the conical bottom of the bioreactor, indicating a potential for such elements to be recovered in biological AMD treatment.

The configuration of the DFSBR bioreactor, based on the immobilization of biomass in its peculiar arrangement of the support material, seems adequate to treat wastewaters containing a high concentration of metals because the precipitated material did not cause clogging of the bed.

This research provides possibilities for DFSBR configuration applications aiming at simultaneous sulfate reduction and the recovery of metal and REY in a single unit, although problems with reactor performance must be overcome in future investigations to allow long-term system operations.

Finally, this is also the first study to describe a sulfidogenic bioreactor treating actual AMD rich in REY and uranium using sugarcane vinasse as the electron donor.

ACKNOWLEDGEMENTS

The authors are very grateful for the financial support provided by PROEX-CAPES (Process 88887.360712/2019-00), FAPEMIG (Process TEC – APQ-02894-14) and FAPESP (2015/06246-7). The authors are also grateful to the *Indústrias Nucleares do Brasil* (INB) for providing acid mine drainage and REY analysis.

REFERENCES

APHA 2005 *Standard Methods for the Examination of Water and Wastewater*, 21th edn. American Public Health Association, Washington, DC, USA.

Ayora, C., Macías, F., Torres, E., Lozano, A., Carrero, S., Nieto, J. M., Pérez-López, R., Fernández-Martínez, A. & Castillo-Michel, H. 2016 Recovery of rare earth elements and yttrium from passive- remediation systems of acid mine drainage. *Environ. Sci. Technol.* **50**, 8255–8262.

Bekmezci, O. K., Ucar, D., Kaksonen, A. H. & Sahinkaya, E. 2011 Sulfidogenic biotreatment of synthetic acid mine drainage and sulfide oxidation in anaerobic baffled reactor. *J. Hazard. Mater.* **189**, 670–676.

Caraballo, M. A., Wantyd, R. B., Verplanckd, P. L., Navarro-Valdivia, L., Ayora, C. & Hochella Jr., M. F. 2019 Aluminum mobility in mildly acidic mine drainage: interactions between hydrobasaluminite, silica and trace metals from the nano to the meso-scale. *Chem. Geol.* **519**, 1–10.

Cravotta III, C. A. 2008 Dissolved metals and associated constituents in abandoned coalmine discharges, Pensylvania, USA. Part I: Constituents quantities and correlations. *Appl. Geochem.* **23**, 166–202.

Falagán, C., Yusta, I., Sánchez-españa, J. & Johnson, D. B. 2017 Biologically-induced precipitation of aluminium in synthetic acid mine water. *Miner. Eng.* **106**, 79–85.

Fuess, L. T., Kiyuna, L. S. M., Garcia, M. L. & Zaiat, M. 2016 Operational strategies for longterm biohydrogen production from sugarcane stillage in continuous acidogenic packed-bed reactor. *Int. J. Hydrogen Energy* **41**, 8132–8145.

Fuess, L. T., Zaiat, M. & do Nascimento, C. A. O. 2019 Novel insights on the versatility of biohydrogen production from sugarcane vinasse via thermophilic dark fermentation: impacts of pH-driven operating strategies on acidogenesis metabolite profiles. *Bioresour. Technol.* **286**, 121379.

Godoi, L. A. G., Damianovic, M. H. R. Z. & Foresti, E. 2015 Sulfidogenesis interference on methane production from carbohydrate-rich wastewater. *Water Sci. Technol.* **72**, 1644–1652.

Godoi, L. A. G., Foresti, E. & Damianovic, M. H. R. Z. 2017a Down-flow fixed-structured bed reactor: an innovative reactor configuration applied to acid mine drainage treatment and metal recovery. *J. Environ. Manage.* **197**, 597–604.

Godoi, L. A. G., Dos Santos, C. E. D., Foresti, E. & Damianovic, M. H. R. Z. 2017b Evaluating and refining alkalinity calculations dueto sulfide and bicarbonate accessed by titration in anaerobic sulfate-reducing bioreactors. *Water Air Soil Pollut.* **228**, 322.

Gonçalves, M. M. M., da Costa, A. C. A., Leite, S. G. F. & Sant'Anna Jr., G. L. 2007 Heavy metal removal from synthetic wastewaters in an anaerobic bioreactor using stillage from ethanol distilleries as a carbon source. *Chemosphere* **69**, 1815–1820.

Hatje, V., Pedreira, R. M. A., Rezende, C. E., Schettini, C. A. F., Souza, G. C., Marin, D. C. & Hackspacher, P. C. 2017 The environmental impacts of one of the largest tailing dam failures worldwide. *Sci. Rep.* **7**, 10706.

Johnson, D. B. & Hallberg, K. B. 2005 Acid mine drainage: remediation options. *Sci. Total Environ.* **338**, 3–14.

Kefeni, K. K., Msagati, T. A. M. & Manba, B. B. 2017 Acid mine drainage: prevention, treatment options, and resource recovery: a review. *J. Clean. Prod.* **151**, 475–493.

Lens, P. N. L., Visser, A., Janssen, A. J. H., Hulshoff Pol, L. W. & Lettinga, G. 1998 Biotechnological treatment of sulfate-rich wastewaters. *Crit. Rev. Environ. Sci.* **28**, 41–88.

Lewis, A. E. 2010 Review of metal sulphide precipitation. *Hydrometallurgy* **104**, 222–234.

Maillacheruvu, K. Y., Parkin, G. F., Peng, C. Y., Kuo, W. C., Oonge, Z. I. & Lebduschka, V. 1993 Sulfide toxicity in anaerobic systems fed sulfate and various organics. *Water Environ. Res.* **65**, 100–109.

Miekeley, N., Coutinho de Jesus, H. & Porto da Silveira, C. L. 1992 Rare earth elements in groundwater from the Osamu Utsumi mine and Morro do Ferro analogue study sites, Poços de Caldas, Brazil. *J. Geochem. Explor.* **45**, 365–387.

Nadaleti, W. C., Lourenço, V. A., Filho, P. B., Santos, G. B. D. & Przybyla, G. 2019 National potential production of methane and electrical energy from sugarcane vinasse in Brazil: a thermo-economic analysis. *J. Environ. Chem. Eng.* (in press).

Niz, M. Y. K., Etchelet, I., Fuentes, L., Etchebehere, C. & Zaiat, M. 2019 Extreme thermophilic condition: an alternative for long-term biohydrogen production from sugarcane vinasse. *Int. J. Hydrogen Energy* **44**, 22876–22887.

Parsaee, M., Kiani, M. K. D. & Karimi, K. 2019 A review of biogas production from sugarcane vinasse. *Biomass Bioenergy* **122**, 117–125.

Reis, M. A. M., Almeida, J. S., Lemos, P. C. & Carrondo, M. J. T. 1992 Effect of hydrogen sulfide on growth of sulfate reducing bacteria. *Biotechnol. Bioeng.* **40**, 593–600.

Rodriguez, R. P., Oliveira, G. H. D., Raimundi, I. M. & Zaiat, M. 2012 Assessment of a UASB reactor for the removal of sulfate from acid mine water. *Int. Biodeter. Biodegr.* **74**, 48–53.

Sánchez-España, J. 2007 The behavior of iron and aluminum in acid mine drainage. In: *Thermodynamics, Solubility and*

Environmental Issues. Elsevier, Amsterdam, The Netherlands, pp. 137–150.

Sánchez-España, J., Yusta, I. & Burgos, W. D. 2016 Geochemistry of dissolved aluminum at low pH: hydrobasaluminite formation and interaction with trace metals, silica and microbial cells under anoxic conditions. *Chem. Geol.* **441**, 124–137.

Sánchez-España, J., Wang, K., Falagán, C., Yusta, I. & Burgos, W. D. 2018 Microbially mediated aluminosilicate formation in acidic anaerobic environments: a cell-scale chemical perspective. *Geobiology* **16**, 88–103.

Santos, A. L. & Johnson, D. B. 2017 The effects of temperature and pH on the kinetics of an acidophilic sulfidogenic bioreactor and indigenous microbial communities. *Hydrometallurgy* **168**, 116–120.

Schlinkert, D. & van den Boogaart, K. G. 2015 The development of the market for rare earth elements: insights from economic theory. *Resour. Policy* **46**, 272–280.

Stewart, B. W., Capo, R. C., Hedin, B. C. & Hedin, R. S. 2017 Rare earth element resources in coal mine drainage and treatment precipitates in the Appalachian Basin, USA. *Int. J. Coal Geol.* **169**, 28–39.

Sun, H., Zhao, F., Zhang, M. & Lin, P. 2012 Behavior of rare earth elements in acid coal mine drainage in Shanxi Province. *China. Environ. Earth Sci.* **67**, 205–213.

U.S. Geological Survey 2019 *Rare Earths*. Mineral Commodity Summaries, U.S. Geological Survey, pp. 132–133. http://minerals.usgs.gov/minerals/pubs/commodity/rare_ earths/.

Villa-Gomez, D., Ababneh, H., Papirio, S., Rousseau, D. P. L. & Lens, P. N. L. 2011 Effect of sulfide concentration on the location of the metal precipitates in inversed fluidized bed reactors. *J. Hazard. Mater.* **192**, 200–207.

Zhao, F., Cong, Z., Sun, H. & Ren, D. 2007 The geochemistry of rare earth elements (REE) in acid mine drainage from the Sitai coal mine, Shanxi Province, North China. *Int. J. Coal Geol.* **70**, 184–192.

Ziemkiewicz, P., He, T., Noble, A. & Liu, X. 2016 Recovery of rare earth elements (REEs) from coal mine drainage. In: *Proc. 37th W. Virginia Surface Mine Drainage Task Force Symposium*, pp. 43–50. In: Thermodynamics, Solubility and Environmental Issues. Elsevier, Amsterdam, The Netherlands, pp. 137–150. https://wvmdtaskforce.com/past-symposium-papers/2016-symposium-papers/.

First received 31 July 2019; accepted in revised form 22 November 2019. Available online 3 December 2019